# Muscle MRI in Duchenne and Becker muscular dystrophy

Wokke, B.H.A.

Chapter 6

# Muscle spectroscopy detects elevated PDE/ATP ratios prior to fatty infiltration in Becker muscular dystrophy patients

*B.H. Wokke, M.H. Hooijmans, J.C. van den Bergen, A.G. Webb, J.J. Verschuuren, H.E. Kan*

**NMR in Biomedicine 2014 Nov 27 (11) 1371-7**

## ABSTRACT

Becker muscular dystrophy is characterized by progressive muscle weakness. Muscles show structural changes (fatty infiltration, fibrosis) and metabolic changes, both of which can be assessed using MRI and MRS. It is unknown at what stage of the disease process metabolic changes arise and how this might vary for different metabolites. In this study we assessed metabolic changes in skeletal muscles of Becker patients, both with and without fatty infiltration, quantified via Dixon MRI and $^{31}$P MRS. MRI and $^{31}$P MRS scans were obtained from twenty-five Becker patients and fourteen healthy controls using a 7T MR scanner. Five lower leg muscles were individually assessed for fat and muscle metabolite levels. In the peroneus, soleus and anterior tibialis muscles with non-increased fat levels PDE/ATP ratios were higher ($p<0.02$) compared to controls, whereas in all muscles with increased fat levels PDE/ATP ratios were higher compared to healthy controls ($p\leq0.05$). The Pi/ATP ratio in the peroneus muscles was higher in muscles with increased fat fractions ($p=0.005$) and the PCr/ATP ratio was lower in the anterior tibialis muscles with increased fat fractions ($p=0.005$). There were no other significant changes in metabolites, but an increase in tissue pH was found in all muscles of the total group of BMD patients in comparison with healthy controls ($p<0.05$). These findings suggest that $^{31}$P MRS can be used to detect early changes in individual muscles of Becker muscular dystrophy patients, which are present before the onset of fatty infiltration.

## INTRODUCTION

Becker muscular dystrophy (BMD) is an X-linked disease caused by mutations in the *DMD* gene, which codes for the dystrophin protein, an important factor for muscle membrane stability [10]. In BMD patients the dystrophin protein is only partially functional, resulting in continuous muscle fiber damage. There is inflammation and oedema in the muscle and eventually the muscle cells' regenerative capacity becomes exhausted and muscle tissue is replaced by adipose and fibrotic tissue [38, 54]. The main feature of the disease is progressive muscle weakness with a limb-girdle distribution, but symptoms can be highly variable in age of onset, severity of symptoms and rate of progression [159, 160]. The underlying mechanisms causing the variability are not fully understood and are thought to include factors like the regenerative capacity of the muscle, quantity of the remaining dystrophin protein and the specific mutation [154-157, 198].

Skeletal muscles of BMD patients show a distinct pattern of fatty infiltration, which can be assessed with magnetic resonance imaging (MRI) [199]. With the progression of the disease the amount of adipose tissue in the muscle increases, and muscles of clinically asymptomatic patients can already show fatty infiltration in some muscles, while others still appear to be normal [199]. In addition to these structural changes in the muscle, several phosphorus MR spectroscopy ($^{31}$P-MRS) studies have reported changes in BMD patients suggestive of an altered energy metabolism [92, 95, 200, 201]. However, the results of these studies have been inconsistent; both unchanged and decreased phosphocreatine (PCr) to adenosine triphosphate (ATP) ratios, increased, unchanged and decreased inorganic phosphate (Pi)/ATP ratios and an unchanged and increased intracellular pH and possibly increased phosphodiesters (PDE)/ATP ratios have been reported [92, 94, 95, 200, 201]. Mitochondrial function is believed to be normal in these patients and it has been suggested that there is reduced glycolytic activity in the skeletal muscles [95, 200]. While structural changes like fatty infiltration and fibrosis are predominantly present in muscles that are in a more advanced stage of the dystrophic process, metabolic changes are thought to occur earlier [202]. However, it is unknown if and how metabolic changes contribute to the muscle degeneration and to what extend these changes are present before the occurrence of fatty infiltration. Previous studies in BMD patients have focused on the more severely affected gastrocnemic muscles using surface coil localization only, without the combination of imaging data and patients with variable disease severity. Therefore it is unknown if the reported changes in phosphorous metabolism in BMD patients are already present in muscles without fatty infiltration, i.e. a less advanced stage of the disease before signs of the dystrophic process are visible with MRI. Since metabolic processes are more likely to be reversible than structural changes like fatty infiltration they could

be valuable as an early marker to evaluate disease progression and possibly effects of future therapeutic interventions [110, 203-205].
In this study, we used high magnetic field quantitative MRI and MRS in BMD patients and healthy controls to assess phosphorous metabolism in five individual lower leg muscles, and correlated the findings to the level of fatty infiltration obtained from the same muscles to assess if metabolic changes vary in different stages of the dystrophic process.

## MATERIALS AND METHODS

### Subjects

All patients were recruited from the Dutch Dystrophinopathy Database. Controls were recruited from the Leiden University Medical Center Radiology database for healthy controls. The diagnosis BMD was confirmed by a mutation in the *DMD* gene or reduced dystrophin expression in a muscle biopsy. BMD patients were classified into four groups according to their clinical functioning: no motor symptoms, mildly affected (patients with difficulty walking and/or difficulty climbing stairs, but not using a walking aid), moderately affected (patients using a walking aid: stick, frame or intermittent wheelchair use), and severely affected patients (completely wheelchair dependent).
The local medical ethics committee approved the study and all study participants gave written informed consent.

### MR examination

Data were acquired on a 7T Philips Achieva MRI (Philips Healthcare, The Netherlands). A custom-built volume birdcage coil (diameter 17.5 cm, length 12 cm) tuned for both proton ($^{1}$H) imaging (higher order mode) and phosphorous ($^{31}$P) spectroscopy (homogeneous quadrature mode) was positioned around the left lower leg directly distal of the patella [206]. Patients were positioned in supine position, feet first, in the scanner. The imaging protocol consisted of an anatomical gradient echo sequence (15 slices; slice thickness 7mm; interslice gap 0.5 mm; repetition time (TR) 10 ms; echo time (TE) 3.0 ms; flip angle (FA) 30°; FOV 180x200 mm) a three-point gradient echo Dixon sequence (12 slices; slice thickness 10 mm; interslice gap 0.5 mm; TR/TE/ΔTE 300/2.4/0.33 ms; FA 30°; FOV 180x204 mm) and a B0 map (14 slices; slice thickness 8 mm, no slice gap; TR/TE 30/3.11ms; FA 20°; FOV 160x180 mm). A 2D phosphorous MRS chemical shift imaging (CSI) dataset was acquired based on the T1-weighted images (FOV 160x200 mm; matrix size 8 x 10; TR 2000 ms; samples 2048; voxel size 20x20 mm; FA 45°; Hamming weighted acquisition with 14 signal averages at

the central k-lines, voxel size after hamming weighing 3.42x3.42 x12 $cm^3$). Second order shimming was performed using an image based shimming routine [207]. As the diameter of the lower leg and the boundaries between the different muscle groups change along the length of the leg, the 2D-CSI sequence was planned in such a way that within the volume of the coil a specific voxel was located within one individual lower leg muscle (Figure 1). The total scan duration was approximately 50 minutes. For quality control of the 7T Dixon data the 7T values were compared to Dixon MRI data acquired from the same patients on a 3T Philips Achieva scanner in a subgroup of 9 patients previously described by Van den Bergen et al. [198]. Data of these patients was obtained on the same day, from the same leg using a 14-cm diameter two-element coil with body coil excitation position directly distal of the patella.

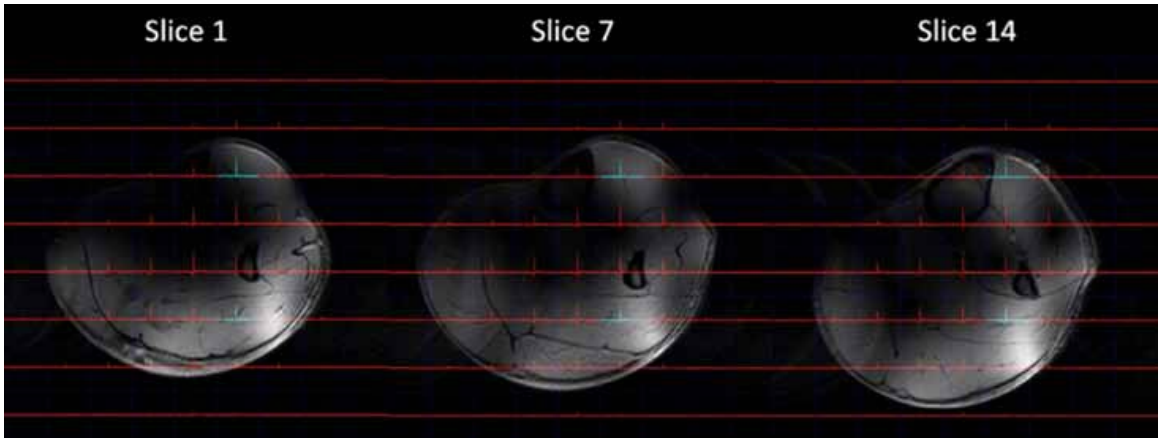


**Figure 1.** Example of the planning of the $^{31}$P 2D-CSI dataset superimposed on an axial T1 weighted image.
The spectroscopy grid was positioned so that specific voxel was located within one individual lower leg muscle over the entire length of the coil: in the first (a.), middle (b.) and last slice (c.) of the T1-weighted image the voxel in the tibialis anterior muscle as well as the voxel in the soleus muscle lies within the same muscle over the length of the coil.



## Data analysis

$^{31}$P Data sets were visualized using the 3D Chemical Shift Imaging package (3DiCSI) and spectra were identified in the tibialis anterior (TA), peronei (PER), soleus (SOL), lateral head of the gastrocnemius (GCL) and medial head of the gastrocnemius (GCM) muscles using a grid overlay on the T1-weighted image (Figure 2). Voxels were carefully positioned to avoid overlap with adjoining muscles.
The free induction decays were exported and fitted using AMARES in jMRUI software package (version 4, http://sermn02.uab.es/mrui). In some patients high amounts of fatty infiltration within the muscle resulted in a low signal-to-noise in the phosphorous spectra due to the very low amount of muscle tissue in the voxel. Consequently only

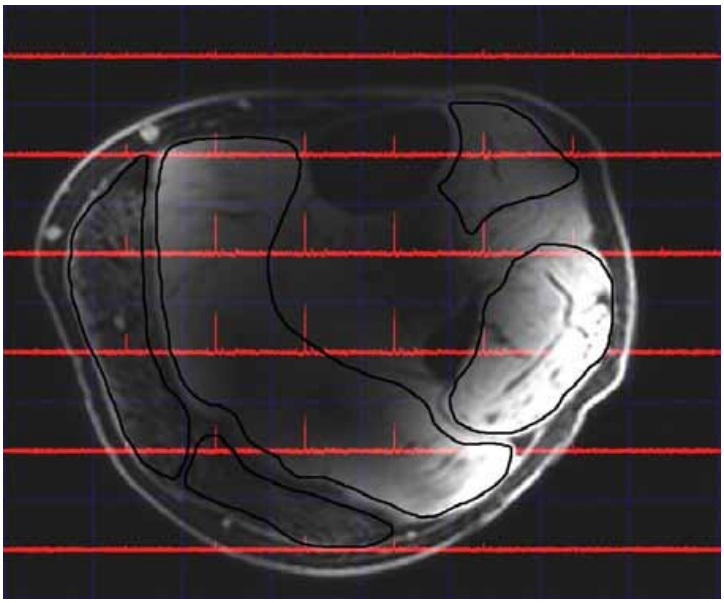

**Figure 2.** Grid overlay on an axial Dixon water-image of the lower leg of a BMD patient.
Spectra were analysed in the anterior tibialis, peroneus, soleus and medial and lateral head of the gastrocnemic muscle for which the ROIs are drawn on the image. Voxels of the CSI-grid were carefully positioned to avoid overlap with adjoining muscles. Note that the coil used for this image is a single tuned birdcage coil, with the primary homogeneous mode being at the phosphorus frequency and a higher mode at the proton frequency, resulting in a loss of sensitivity in the center of the coil for proton, but not for phosphorous.

the muscles with an acceptable quality spectrum (i.e. SNR greater than 10 for the PCr peak in combination with the ability to identify all other metabolite signals and with percentage Cramér-Rao Lower Bound (CRLB) values for all fitted metabolites below 20%) were included in the analysis. Signals of Pi, PDE, PCr and γ-, α- and β-ATP were fitted with Gaussian line shapes (Figure 3). For the PDE and β-ATP peak prior knowledge on the line width was used. The line width for PDE was set at 1.3* the line width of PCr and the β-ATP line width was set at 1.6* the line width of α-ATP, this prior knowledge was based on the mean line widths of 10 patients with high SNR. Metabolite ratios were obtained from Pi, PDE and PCr relative to the γ- ATP signal and corrected for $^{1}$H relaxation effects measured in human calf muscle at 7T assuming the same relaxation parameters for all muscles [208]. Intracellular tissue pH was calculated from the shift in resonance position (S) of the Pi peak compared to PCr: pH=6.75 + log ((3.27-S)/(S-5.69)) [209].
Quantitative fat fractions of the muscles were calculated from the Dixon MR images using Medical Image Processing, Analysis and Visualization (MIPAV) software (http://mipav.cit.nih.gov). Regions of interest (ROIs) were drawn on all slices, on the same muscles as used for the spectroscopy analysis. Fat fractions were calculated as signal intensity (SI) fat/ (SI fat+ SI water))*100. 3T values were corrected for relaxation effects as described before [143]. For the comparison of 3T and 7T data, fat fractions

obtained from the TA, PER, SOL, GCL and GCM muscles from a similar number of slices from both scanners were compared on a muscle-by-muscle basis.
All individual muscles of the Becker patients were classified into two groups according to the level of fatty infiltration compared to healthy controls; BMD with non-increased fat levels (NIFL)), and BMD with increased levels of fatty infiltration (IFL). Cut-off values were calculated for the five individual lower leg muscles using mean+2 standard deviations (SD) of the fat fraction of the corresponding lower leg muscle of healthy controls.

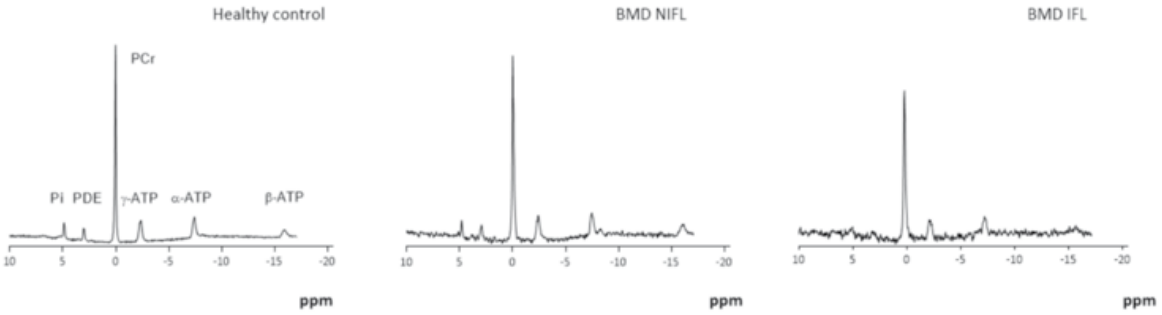


**Figure 3.** Representative phosphorous 7T spectra of the peroneus muscle in a healthy control, BMD patient with non-increased fat fractions (BMD NIFL) and BMD patient with increased fat fractions (BMD IFL).
Spectra are scaled to the ATP levels. The signal to noise ratio of the 31P signal clearly decreases in the BMD patient with increased fat levels. Peak assignments Pi = inorganic phosphate, PDE = phosphodiester, PCr = phosphocreatine, γ-, α- and β-ATP = three resonances of adenosine triphosphate.

## Statistics

For the comparison of the metabolite ratios Pi/ATP, PCr/ATP, PDE/ATP, Pi/PCr and pH between the groups for the five lower leg muscles two general linear models were used, one for the comparison of healthy controls with the whole group of BMD patients and one for the comparison of healthy controls with the NIFL BMD and IFL BMD groups. Age was entered as a covariate and disease as a fixed factor. A Fischer LSD model was used to correct for multiple comparisons. Pearson correlation was used for the comparison of the Dixon scan data acquired at 3T and 7T to explore the relation between fat fractions and the PDE/ATP ratio in both healthy controls and BMD patients. The level of significance was set at $P \leq 0.05$. Statistical analysis was performed using SPSS version 20 for Windows (SPSS Inc., Chicago).

## RESULTS

### Patient characteristics

Twenty-five male BMD patients (age 39.6 ± 13 years, range 20-66, BMI 25.04 ± 3.65, range 20-33) and fourteen age-matched healthy male controls (age 35.7 ± 15 years, range 22-65, BMI 22.64 ± 3.37 range: 20-32.4) participated in the study. All subjects completed the scanning protocol. Of the 25 BMD patients five patients had no motor symptoms, eleven were mildly affected, seven moderately affected and two severely affected (Table 1). Four of the patients with no motor symptoms showed normal fat levels on Dixon MRI and one patient with no motor symptoms showed a slightly increased fat fraction in the GCM and GCL. The GCM and GCL showed increased fat levels in all moderately affected patients and fat fractions were increased in all investigated muscles of severely affected patients (Table 1).

### Fatty infiltration

The mean fat level in healthy controls was 2.9 ± 1.1% and in patients 16.0 ± 18.6%. Overall the GCM showed the highest mean fat fractions and the SOL the lowest. Muscles with fat fractions lower than the mean fat fraction plus 2 SD in the corresponding muscle of healthy controls were defined as muscles with no significant increase in fatty infiltration and classified in the non-increased fat levels (NIFL) group. The other muscles were classified in the group with increased levels of fatty infiltration (IFL), as compared to healthy controls (Table 1). The fat fractions calculated from five muscles of nine BMD patients acquired at 3T and 7T showed a high correlation (R=0.97).

### $^{31}$P data

All metabolite ratios of the healthy controls and BMD patients are shown in Table 2. For the analysed muscles the NIFL/IFL subgroups were divided as follows; GCL NIFL n=5/IFL n=13 (cut-off fat fraction 3.4%), GCM NIFL n=5/IFL n=9 (cut-off 4.5%), PER NIFL n=10/IFL n=15 (cut-off 6.8%), SOL NIFL n=10/IFL n=15 (cut-off 4.9%), TA NIFL n=18/IFL n=7 (cut-off 8.1%). Due to the high number of patients with increased fat levels in the GCL and GCM muscles, the number of included spectra in the NIFL was lower compared to the other muscles. In addition, for the GCM muscle 11 spectra and seven spectra for the GCL muscle did not meet our quality control criteria and therefore were not included in the analysis. In healthy controls all the acquired spectra were included in the analysis.

For the whole group of BMD patients PDE/ATP ratios were significantly increased compared to healthy controls in all five lower leg muscles. In the NIFL BMD group PDE/ATP ratios were significantly increased compared to healthy controls in the PER, SOL and TA muscles, except for a trend in the GCL (p=0.071) and no significant change

**Table 1.** Patient parameters.

| Patient | Age (years) | Mutation | Age of first symptoms | Disability | Non-increased fat levels muscles |
|---|---|---|---|---|---|
| 1 | 56 | Unknown* | 35 | Mild | PER, TA |
| 2 | 48 | Del45-48 | 14 | Moderate | None |
| 3 | 49 | Del45-48 | 10 | Moderate | None |
| 4 | 29 | Exon 19 c.2380+3A>C ** | 4 | Severe | None |
| 5 | 51 | Del45-55 | 6 | Mild | PER, SOL, TA |
| 6 | 63 | Del45-55 | 40 | Mild | TA |
| 7 | 30 | p1172X | 4 | Mild | TA |
| 8 | 26 | Del45-47 | 9 | No motor symptoms | GCL, GCM, PER, SOL, TA |
| 9 | 38 | Exon 29 p.Arg131>X *** | None | No motor symptoms | GCL, GCM, PER, SOL, TA |
| 10 | 24 | Del30-44 | 12 | Mild | TA |
| 11 | 63 | Del45-47 | 10 | Severe | None |
| 12 | 33 | Del03-05 | None | Mild | TA |
| 13 | 66 | Dup14-42 | 6 | Moderate | None |
| 14 | 39 | Del45-47 | 6 | Mild | None |
| 15 | 37 | Del45-47 | 3 | Moderate | SOL, TA |
| 16 | 20 | Del45-47 | None | No motor symptoms | GCL, GCM, PER, SOL, TA |
| 17 | 29 | Del45-47 | 12 | Mild | PER, TA |
| 18 | 39 | Del45-47 | 15 | Mild | TA |
| 19 | 31 | Del03-04 | 18 | Moderate | PER, SOL, TA |
| 20 | 25 | Del48-49 | Floppy infant | No motor symptoms | GCL, GCM, PER, SOL, TA |
| 21 | 37 | Del03-04 | 3 | Moderate | TA |
| 22 | 33 | Del45-47 | 3 | Mild | GCL, SOL, TA |
| 23 | 42 | Del48-49 | 6 | No motor symptoms | PER, SOL, TA |
| 24 | 43 | Del45-47 | 4 | Moderate | None |
| 25 | 31 | Del45-47 | 2 | Mild | GCL, GCM, PER, SOL, TA |

Disability is scored as no motor symptoms, mild (difficulty walking without the use of walking aid), moderate (use of walking aid) or severe (wheelchair dependent). The muscles with non-increased fat fractions as compared to healthy controls are shown for each patient (medial and lateral head of gastrocnemic muscle (GCL and GCM), soleus (SOL), peroneus (PER) and anterior tibialis (TA)).(*No mutation could be found, patient had been found to have 62% dystrophin. **As a result of this mutation a large part of exon 19 is skipped. ***As a result of this mutation exon 29 is skipped)

in the GCM (p=0.404) (Figure 4). The IFL BMD subgroup showed significantly increased PDE/ATP ratios compared to healthy controls in all lower leg muscles. Values of Pi/ATP, Pi/PCr and PCr/ATP showed no significant differences between the whole group of BMD patients and healthy controls, except for an increase in the Pi/ATP ratio in the PER muscle of BMD patients.

| | Controls | BMD total | BMD NIFL | BMD IFL |
|---|---|---|---|---|
| **GCL** | n=14 | n=18 | n=5 | n=13 |
| Pi/ATP | 0.34±0.02 | 0.40±0.02 | 0.37±0.04 | 0.41±0.03 |
| Pi/PCR | 0.10±0.01 | 0.10±0.01 | 0.09±0.016 | 0.11±0.01 |
| PDE/ATP | 0.19±0.03 | 0.34±0.03* (p=0.001) | 0.288±0.051 | 0.36±0.03* (p=0.001) |
| PCr/ATP | 3.59±0.12 | 3.54±0.11 | 3.842±0.204 | 3.4±0.13 |
| pH | 7.02±0.01 | 7.05±0.01*(p=0.017) | 7.05±0.014 | 7.06±0.01*(p=0.017) |
| **GCM** | n=14 | n=14 | n=5 | n=9 |
| Pi/ATP | 0.38±0.03 | 0.44±0.03 | 0.42±0.04 | 0.45±0.03 |
| Pi/PCR | 0.10±0.05 | 0.18±0.05 | 0.11±0.08 | 0.22±0.06 |
| PDE/ATP | 0.25±0.04 | 0.34±0.04*(p=0.046) | 0.27±0.06 | 0.38±0.05*(p=0.036) |
| PCr/ATP | 3.82±0.16 | 3.77±0.16 | 3.81±0.27 | 3.76±0.20 |
| pH | 7.02±0.01 | 7.05±0.01*(p=0.025) | 7.04±0.01 | 7.05±0.01*(p=0.033) |
| **PER** | n=14 | n=25 | n=10 | n=15 |
| Pi/ATP | 0.32±0.03 | 0.40±0.02*(p=0.016) | 0.36±0.03 | 0.43±0.03*(p=0.005) |
| Pi/PCR | 0.09±0.01 | 0.11±0.006 | 0.11±0.01 | 0.12±0.01*(p=0.035) |
| PDE/ATP | 0.16±0.03 | 0.33±0.02*(p<0.001) | 0.30±0.032*(p=0.003) | 0.35±0.03*(p<0.001) |
| PCr/ATP | 3.48±0.1 | 3.61±0.07 | 3.53±0.11 | 3.66±0.09 |
| pH | 7.01±0.01 | 7.02±0.01*(p=0.047) | 7.02±0.01 | 7.02±0.01 |
| **SOL** | n=14 | n=25 | n=10 | n=15 |
| Pi/ATP | 0.38±0.02 | 0.40±0.02 | 0.40±0.03 | 0.40±0.024 |
| Pi/PCR | 0.11±0.01 | 0.12±0.01 | 0.13±0.011 | 0.11±0.01 |
| PDE/ATP | 0.21±0.03 | 0.34±0.02*(p=0.003) | 0.33±0.04*(p=0.017) | 0.34±0.03*(p=0.006) |
| PCr/ATP | 3.57±0.11 | 3.65±0.08 | 3.52±0.13 | 3.73±0.10 |
| pH | 7.02±0.01 | 7.04±0.004*(p=0.006) | 7.04±0.01 | 7.04±0.01*(p=0.006) |
| **TA** | n=14 | n=25 | n=18 | n=7 |
| Pi/ATP | 0.35±0.03 | 0.37±0.02 | 0.40±0.02 | 0.29±0.036 |
| Pi/PCR | 0.10±0.01 | 0.10±0.01 | 0.11±0.01 | 0.09±0.01 |
| PDE/ATP | 0.17±0.04 | 0.30±0.03*(p=0.01) | 0.30±0.03*(p=0.019) | 0.30±0.05* (p=0.05) |
| PCr/ATP | 3.66±0.12 | 3.53±0.1 | 3.71±0.102 | 3.06±0.16(p=0.005) |
| pH | 7.00±0.01 | 7.02±0.01*(p=0.039) | 7.01±0.01 | 7.02±0.01 |

**Table 2.** Mean values ±SD for the different metabolites in healthy controls, the overall BMD group, BMD patients with non-increased fat levels (NIFL) and BMD patients with increased fat levels (IFL). Significant differences between patients and controls are marked with an asterisk (*) and for these p values are shown. (Pi = inorganic phosphate, PDE = phosphodiester, PCr = phosphocreatine, ATP=adenosine triphosphate. GCL/GCM= lateral and medial head gastrocnemius, PER= peroneus, SOL=soleus, TA=anterior tibialis).

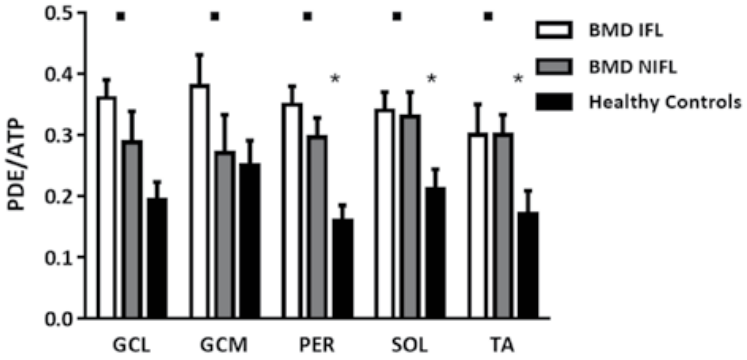


**Figure 4.** Mean phosphodiester (PDE) in medial and lateral gastrocnemic muscle (GCL and GCM), peroneus (PER), soleus and anterior tibialis (TA) in healthy controls (black), BMD patients with non-increased fat levels (NIFL) (white) and BMD patients with increased fat levels (IFL) (grey).
Ratios significantly higher in BMD NIFL compared to controls are shown with an asterix (*) and significantly higher in BMD IFL compared to control with a square (•). P values are as follows: for the NIFL BMD group (GCL p= 0.071, GCM p= 0.404, PER p= 0.003, SOL p=0.017 and TA p=0.019) and in the IFL BMD group (GCL p=0.001, GCM p=0.036, PER p<0.001, SOL p=0.006 and TA p=0.05).

In the NIFL BMD group no significant differences were found for any of these metabolites (Table 2). Therefore, the increase in Pi/ATP ratio in the PER of the overall BMD group is due to the IFL BMD group in which significant increases in the Pi/ATP (p=0.005) and Pi/PCr (p=0.035) were found for the PER. There was a significant increase in tissue pH in the GCM, GCL and SOL muscle in the IFL group, as well as in all muscles of the whole BMD group. Additionally there was a significant correlation between the fat fraction and PDE/ATP ratio in the BMD patients (R=0.20, p=0.04), but not in healthy controls (R=-0.02, p=0.9) (Figure 5).



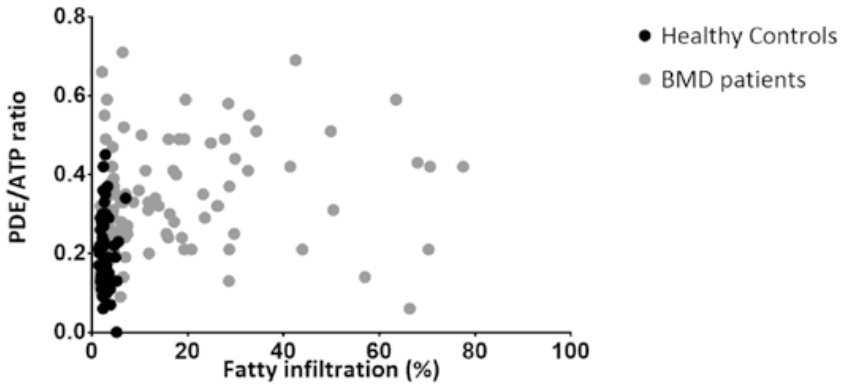


**Figure 5.** Correlation between PDE/ATP ratios and fatty infiltration in BMD patients (grey dots) and healthy controls (black dots).
For BMD patients there is a low, but significant correlation (R=0.20, p=0.04), however in the higher fat fractions PDE/ATP ratios show great variability.

## DISCUSSION

In this study we used a combination of quantitative proton MRI and localized $^{31}$P MR spectroscopy to evaluate high-energy phosphate levels in five lower leg muscles of BMD patients. In BMD patients the SOL, PER and TA with non-increased fat fractions and all muscles with increased fat fractions showed increased PDE/ATP ratios. This suggests that $^{31}$P MRS can be used to detect changes muscles of BMD patients before the onset of potentially irreversible changes like fatty infiltration.

The PDE signal in the MR spectrum is derived from glycerol 3-phosphocholine (GPC) and glycerol 3-phosphoethanolamine (GPE) which are thought to be membrane phospholipids breakdown products [210, 211]. Slow-twitch, oxidative type 1 fibers have been shown to have higher PDE/ATP ratios and PDE has also been shown to increase with age [212, 213]. In addition, GPCs have been suggested to have some regulatory effects [214-217]. In muscular dystrophies increased PDE/ATP ratios have been found in Golden Retriever muscular dystrophy (GRMD) dogs, in Duchenne muscular dystrophy (DMD) patients, and in moderately affected BMD patients [95, 96, 112, 201, 218]. Our results are in agreement with these studies, although we did not find an increase in PDE/ATP ratio in the GCM and a trend in the GCL muscle. However, as we only had five data points in the NIFL group in these muscles, this could have resulted from a failure to reach statistical significance for these muscles. On the other hand, the SOL, PER and TA have a higher percentage of type 1 muscle fibers, and it could be that they are in some way affected differently by the ongoing membrane damage [210, 219]. As dysfunctional or absent dystrophin results in muscle membrane instability the elevated PDE/ATP ratios may also directly reflect membrane damage [220]. This is supported by the fact that in facioscapular muscular dystrophy (FSHD), a muscular dystrophy with no primary membrane damage, increased PDE/ATP ratios were only found in patients with increased fat levels [221]. However, the finding that in DMD patients fast, glycolytic type 2 fibres are preferentially affected could give some support the theory of a more regulatory role of PDE [112, 214, 217].

In previous studies where $^{31}$P MRS was applied in BMD patients only the (posterior) calf muscles of mild to moderately affected patients were scanned, without direct comparison with imaging data. As a result, no data were available on muscles without fatty infiltration and it was not clear if changes in phosphorous signals were already present before the onset of fatty infiltration. This is important, as PDE/ATP ratios have been shown to be adaptable in some conditions, whereas substitution of adipose tissue by muscle fibers has to our knowledge never been reported [110, 203-205, 222]. As it is likely that increased PDE/ATP ratios are to some extend related to muscle membrane damage, they could potentially be a marker for therapy efficacy if therapies preventing the membrane damage become available.

The GCM, GCL and SOL with IFL showed a more alkaline pH than controls, which is in accordance with results of mild to moderately affected BMD patients from previous studies [92, 200, 201]. When evaluating the whole BMD group an increased pH was found for all investigated muscles. The cause for the increased pH, although frequently observed in BMD and DMD patients, is unclear. Possibly factors related to mitogenesis or an altered sarcolemmal proton efflux mechanisms ion transport are involved [95, 223].

We found no consistent changes in Pi/ATP or PCr/ATP ratios in the investigated muscles. The fact that we did not find an increased Pi/ATP ratio and decreased PCr/ATP ratio in gastrocnemic muscles as reported in some previous studies could be related to the fact that we had to discard some of the spectra of severely affected patients, as they were of insufficient quality to analyse [92, 224]. This may have somewhat biased our results with regards to these muscles.

Our study has some limitations, as mentioned above we had to discard some of the spectra of the gastrocnemic muscles of BMD patients as they were of insufficient quality to be used for the analysis. This could have resulted in a bias with regards to the findings in the more severely fatty infiltrated gastrocnemic muscles and possibly be an explanation why no significant abnormalities were found in Pi/ATP and PCr/ATP ratios in these muscles. Secondly the NIFL groups for the gastrocnemic muscles were relatively small compared to the control group. As these muscles are the most severely affected in the lower leg of BMD patients this is not unexpected, however, it might have influenced the findings in terms of PDE levels and possibly the other metabolites in these muscles. Thirdly, the use of a 2D-CSI sequence instead of 3D could potentially result in a voxel spanning different muscles along the length of the leg. To circumvent this problem the 2D-CSI spectroscopy grid was carefully planned so that one voxel of each of the analysed muscles was located within the specific muscle, as demonstrated in Figure 1. If it was not possible to allocate the voxel solely to a specific muscle, due to the muscle being too small, the voxel was positioned in such a way that either air or bone (tissue from which no phosphor signal could be obtained) was included. Finally, the 7T fat fractions were not corrected for relaxation effects, which could have affected the exact fat percentage. However, as fat percentages were calculated using the exact same procedure for patients and age-matched controls, values of healthy controls were used for a muscle specific cut-off value and 3T and 7T values showed a high correlation, this is not likely to have significantly influenced our results.

In conclusion, our results show that MR spectroscopy can detect increased PDE/ATP ratios in lower leg muscles of BMD patients prior to fatty infiltration. Therefore, PDE/ATP ratios could be a useful parameter in the follow-up of muscle membrane damage in early stages of the disease, before more structural changes become apparent.